Tail-end amphiphilic dimethylaminopyridinium-containing polymethacrylates for gene delivery

Pascal Y. Vuillaume,†*[a] Mélanie Brunelle,[a] C. Géraldine Bazuin,[b] Brian G. Talbot,[c] André Bégin,[d] Marie-Rose Van Calsteren[d] and Sylvette Laurent-Lewandowski[a]

Received (in Montpellier, France) 28th April 2009, Accepted 28th July 2009
First published as an Advance Article on the web 7th August 2009
DOI: 10.1039/b908419c

Amphiphilic dimethylaminopyridinium alkyl polymethacrylates (aPPs) were tested for gene complexation, cell cytotoxicity and *in vitro* gene expression for use as gene delivery agents. The aminopyridinium groups neutralized by bromide or octylsulfonate counterions were terminal moieties of side-chain spacers containing 8, 12 or 16 methylene units. This investigation measured the impact of the spacer length and the chemical nature of the counterion on the physicochemical properties and biological activity of the polyplexes formed by the complexation with DNA. The aPPs self-assembled with DNA by neutralizing the DNA phosphate charges through the pyridinium moieties. The degree of DNA condensation was higher for shorter spacer (n = 8, 12) and bromide-neutralized aPPs. Several aPP–DNA complexes formed well-defined nanoparticles, which were usually, but not always, positively charged. Their sizes ranged from 30 to 150 nm and in some cases had an internal lamellar structure visible by TEM. All of the aPPs were found to be much less cytotoxic than branched poly(ethyleneimine) [(PEI), 25 kDa]. The degree of cytotoxicity of the aPPs depended mildly on their spacer length and counterion: a longer spacer (n = 16) decreased the cell viability more than shorter spacers and, at the highest aPP concentrations tested, bromide counterions more than octylsulfonate counterions. The transfection efficiency also depended on the spacer length and counterion type. Polyplexes obtained from the bromide-neutralized aPPs with the n = 12 spacer at an aPP/DNA weight ratio of 2.5, for which negatively charged nanoparticles were formed, were found to be as efficient as PEI-based polyplexes. Interestingly, this demonstrates that endosomolytic fragments and positively charged polyplex surfaces are not required for efficient gene expression.

Introduction

In a few decades, gene therapy may well be a routine tool for the treatment of genetic diseases. The success of such therapy is related to the efficiency of the delivery of DNA encoding the therapeutic proteins. Viral vectors are the most efficient gene delivery systems developed to date, owing to their high capacity for the physical condensation of genetic material within the virus capsid, together with their efficient infection mechanisms. However, viruses also present serious recombination. Many investigations have been carried out to design safe and versatile synthetic carriers with viral-like transfection efficiencies. Amphiphilic block copolymers,[1] cationic polymers,[2,3] non-condensing polymers[4,5] and also a large number of surfactants[6] with different molecular structures (gemini[7] and bolaforms[8,9]) have been tested. Several models of the relationship between structure and biological properties have been proposed.[6]

At first sight, amphiphiles (lipids and surfactants) appear promising as gene delivery systems, but they are often accompanied by undesirable cytotoxicity due to destabilization of the cell membrane caused by their hydrophobic domains.[10] On the other hand, highly ionic polymers and peptides can be effective gene condensing agents and delivery systems.[11] However, these compounds are relatively cytotoxic, related in part to their high cationic charge density.[12,13] The cationic charges, which are needed for efficient DNA condensation, and hydrophobic domains, which promote membrane interaction, have been combined in hydrophobically-modified poly(ethyleneimine) (PEI), poly(L-lysine) (PLL), poly(amidoamine) (PAMAM) and poly(*N*-ethyl-4-vinylpyridinium) salts (PEVP).[13–17] In some cases, this strategy has successfully reduced toxicity without strongly affecting transfection efficiency.[18] In other instances, the most hydrophobic poly(β-amino ester)s, among a large library of molecules, have been found to be the most toxic.[19] Also, PAMAMs with a head-tail geometry, where positive charges (“heads”) are located within or close to the

[a] *Université de Montréal, Faculté de Médecine Vétérinaire, Département de Pathologie et Microbiologie, 3200 rue Sicotte, Saint-Hyacinthe, Québec, Canada J2S 2M2. E-mail: pvuillaume@cegepth.qc.ca; Tel: +1 418 338-6410*
[b] *Université de Montréal, Faculté des Arts et des Sciences, Département de Chimie, C.P. 6128 Succ. Centre-Ville, Montréal, Québec, Canada H3C 3J7*
[c] *Université de Sherbrooke, Faculté des Sciences, Département de Biologie, 2500 boul. de l'Université, Sherbrooke, Québec, Canada J1K 2R1*
[d] *Agriculture et Agroalimentaire Canada, Centre de Recherche et de Développement sur les Aliments, 3600 boul. Casavant Ouest, Saint-Hyacinthe, Québec, Canada J2S 8E3*
† Current address: Centre de Technologie Minérale et de Plasturgie inc., 671, boul. Frontenac Ouest, porte 8, Thetford Mines, Québec, Canada G6G 1N1.

polymer backbone and covalently linked to aliphatic or lipid-like side chains (“tails”), have been found to be quite cytotoxic.[13] On the other hand, no polymers with a tail-end geometry, where the charges are covalently attached to the end of the aliphatic side chains,[20] have so far been investigated for their transfection properties and cytotoxicity.

In the field of cationic amphiphiles designed for gene transfer, those incorporating heterocyclic pyridinium moieties have attracted particular attention, owing to their low cytotoxicity and high transfection efficiency.[21–28] By way of contrast, polycations incorporating amphiphilic pyridinium-containing segments have been far less investigated. Compared to small cationic amphiphiles, the advantage of polymers with a high cationic density is their condensation of DNA into small particles and their ability to form stable complexes with DNA. In this paper, we report on amphiphilic aminopyridinium-containing polymethacrylates (aPPs) with tail-end geometries and a relatively low cationic content as potential low-cytotoxic gene delivery candidates. The thermotropic properties of these types of cationic tail-end polyamphiphiles have been described previously.[29–31] Here we focus on the physicochemical and biological properties of poly(ω-dimethylaminopyridinium alkylmethacrylate)s with octyl, dodecyl and hexadecyl spacers neutralized by bromide (Br) and octylsulfonate (S8) counterions (see Fig. 1). These compounds are referred to by the acronym P*n*DMAP-X, where P, *n*, DMAP and X refer to the polymethacrylate backbone, the number of methylene units in the side chain spacer, the dimethylaminopyridinium cationic group and the type of counterion (Br or S8), respectively. We investigated, in particular, the influence of the spacer length and the chemical nature of the counterion on the specified properties.

Experimental section

Materials and methods

Sterile water (DNase/RNase free, molecular biology reagent), PEI (25 kDa, branched) and ethidium bromide were obtained from Sigma-Aldrich (Oakville, ON). Cell culture plastics were purchased from Corning Costar (Corning, NY). Zeocin, pBudCE4.1/LacZ/CAT plasmid (8433 bp) encoding β-galactosidase under the control of the CMV promoter and *Escherichia coli* Top 10 chemically competent cells were obtained from Invitrogen (Burlington, ON). Dulbecco’s modified Eagle’s medium (DMEM) and OPTI-MEM I reduced serum medium were purchased from GIBCO Invitrogen (Burlington, ON). Fetal bovine serum (FBS) was obtained from Medicorp (Montreal, QC). The COS7 cell line (Simian virus 40-transformed kidney cells of an African green monkey) was obtained from the American Type Culture Collection (ATCC) (Valencia, CA). The MTT cell proliferation kit [3-(4,5-dimethylthiazol-2-yl)-2,5-diphenyltetrazolium] and the β-galactosidase ELISA kit were purchased from Roche Diagnostics GmbH (Laval, QC).

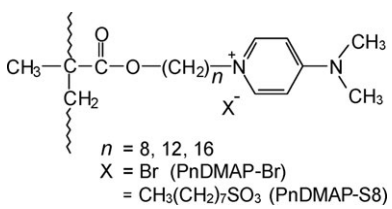

Fig. 1 The chemical structures and acronyms of the bromine- and octylsulfonate-neutralized dimethylaminopyridinium poly(alkyl methacrylate)s studied.

Synthesis of the polyamphiphiles

The synthesis and characterization of the aPPs is described elsewhere.[29–31] In contrast to P8DMAP-Br and P12DMAP-Br, P16DMAP-Br was polymerized in the presence of a small amount of the transfer agent 2-mercaptoethanol to reduce the molar mass, in order to improve the polymer solubility for subsequent ion exchange. The molar mass of the aPPs could not be determined with precision due to the amphiphilic character of these polymers.[29–31] However, they are estimated to be above 10 000 (medium to high molar mass range) based on the absence of NMR signals from chain end groups and on recent NMR and osmometry investigations of similar low molar mass aPPs (see the comments in ref. 31).

Preparation of the polyamphiphile/DNA complexes

Plasmid pBudCE4.1/LacZ/CAT was amplified and used for all the experiments, as described elsewhere.[13] Polyplexes were prepared at different weight ratios (aPP/DNA w/w) with a final DNA concentration of 10 μg mL^{-1} in sterile water. In each case, considering the desired aPP/DNA w/w ratio, an appropriate amount of aqueous polyamphiphile solution (0.5 mg mL^{-1}) was added to the final 500 μL volume of water, and this was gradually added to an appropriate amount of the aqueous DNA solution (20 μg mL^{-1}), with a vortex time of 30 s between each addition. The final solution was stirred for 2 min and incubated at room temperature for 15 min to improve stabilization.

Gel electrophoresis

A control DNA solution or 40 μL of polyplex, both containing 400 ng of DNA, was mixed with bromophenol blue in glycerol, after which they were subjected to electrophoresis on a 0.8% (w/v) agarose gel [tris–acetate–EDTA buffer (pH 8.5), 90 V, ;90 min]. DNA bands were visualized by UV illumination after coloration with ethidium bromide (0.5 μg mL^{-1}) for 30 min. Complete neutralization of the charges on the DNA resulted in its immobilization in the loading well of the gel.

Size distribution and zeta (ζ) potential measurements

The polyplexes were prepared at different weight ratios under conditions identical to those employed for the gel electrophoresis experiments. The sizes, size distributions and ζ-potentials were measured by dynamic light scattering (DLS) on a Zetasizer (Malvern, NanoZS ZEN3600) instrument using the same disposable cell (folded capillary cell DTS 1060). The instrument was equipped with a monochromatic coherent helium neon laser (633 nm) light source. The scattered light was recorded at an angle of 173°, and analysis of the autocorrelation function was performed automatically to yield the diffusion coefficient, DT, using values of 1.33 and 25 °C for the refractive index and temperature, respectively. The intensity and number

distributions were obtained relative to the hydrodynamic diameter using a unimodal distribution. The tail of the correlation function was also examined to determine if aggregates were present. The average particle sizes and standard deviations are given as the mean of six measurements. The ζ-potential was calculated using the Schmoluchowsky approximation[32] and carried out directly after the particle size measurements. Mean ζ-potentials were obtained from three determinations per sample.

Transmission electron microscopy (TEM)

Selected aPPs and polyplexes with weight ratios (w/w) varying from 1 to 5 (P*n*DMAP-Br series) and 10 (P*n*DMAP-S8 series) (prepared as described above) were chosen for morphological investigations. 10 μL of sample was deposited on a 150-mesh copper grid coated with Formvar, followed by careful removal of excess solution using the edge of a moist filter paper. Samples were then negatively stained for 2 min with a droplet of 1% uranyl acetate (aqueous solution, pH 4.5). After removal of the excess stain solution with a moist filter paper, the grid was air dried. Observations were made using a Phillips EM 410 at 80 kV.

Cytotoxicity assays

The metabolic activity of viable COS7 cells was measured using the MTT Cell Proliferation Assay kit 24 h after the incubation of cells with various P*n*DMAP-X concentrations (1.5 to 22.5 μg mL^{-1}). These concentrations corresponded to the quantity of polymer used in the transfection experiments. Cells were grown in 96-well plates for 24 h before treatment at an initial seeding density of 1.9×10^4 cells $well^{-1}$ in 100 μL of complete medium. Various concentrations of P*n*DMAP-X were directly prepared in OPTI-MEM I without serum and applied on the cells. Cells were grown for 24 h in the presence of P*n*DMAP-X and then tested for metabolic activity. MTT reagent (10% v/v) was added to each well (final concentration 0.5 mg mL^{-1}). After 4 h of incubation at 37 °C, the purple insoluble salt was dissolved by adding 100 μL of "solubilization solution". The plate was incubated in the dark at 37 °C for 24 h. The absorbance was measured at 550 nm using a reference wavelength of 650 nm. The viability of cells treated with DNA alone was used as the relative 100% cell viability. The results were expressed as the relative percentage of cell viability relative to the untreated control: Relative cell viability (%) = $(OD_{(550–650)\ sample}/OD_{(550–650)\ naked\ DNA}) \times 100$. PEI cytotoxicity was also evaluated for comparison purposes using equivalent concentrations. Experiments were performed in triplicate.

Transfection protocol

The day preceding the transfection experiment, COS7 cells were seeded on a 6-well plate at a density of 2.9×10^5 cells $well^{-1}$ in a complete medium [90% (v/v) DMEM-containing L-glutamine, 10% FBS] at 37 °C in 5% CO_2 (v/v) to reach 90% confluence at the moment of transfection. Polyplexes were prepared as described above at w/w ratios varying between 1 and 5. Immediately before the transfection experiment, the medium was removed. The cells were washed twice with phosphate-buffered saline (PBS), and then 1 mL of serum-free OPTI-MEM I medium, followed by the polyplex solution (500 μL, 5 μg of DNA $well^{-1}$), was added to the cells. These serum-free transfection mixtures were incubated for 4 h, after which the medium was replaced with complete medium for 20 h. The β-galactosidase content was determined using the ELISA kit. Total protein content was determined by a bicinchoninic acid assay (BCA) from Pierce. Results are expressed as pg of β-galactosidase per μg of total protein. Negative and positive transfection controls were performed using naked DNA (5 μg) and PEI polyplexes (at a PEI/DNA N : P ratio of 10),[8] respectively. Transfection experiments were repeated three times.

Results and discussion

Charged site and stability characteristics of P*n*DMAP-X

Tail-end P*n*DMAP-X polyamphiphiles bear aliphatic side chains with terminal groups that possess two kinds of amino moieties. One is a quaternary ammonium that forms part of the pyridinium heterocycle, the other is a tertiary amine tail linked directly to the heterocycle. The former is permanently charged, whereas the latter was found not to be protonated under physiological conditions, nor under much more acidic conditions (pH $\sim$ 1), probably due to the electron withdrawing effect of the pyridinium group and the delocalization of the charge over the aromatic ring, both of which decrease the basicity. The acid dissociation constant (pK_a) of the tertiary amine was estimated using the ACD/Labs calculator program for a methacrylic dimer with unpolymerized double bonds (neglecting any resonance effects). The negative pK_a value obtained (−4.1) is in agreement with the value (−4.4) reported elsewhere.[33] ^{1}H NMR chemical shift data, which showed no change with varying pH, also indicate that there is no protonation of the tertiary amine under acidic conditions (pH $\sim$ 1). These results confirm that the exocyclic DMAP nitrogen is virtually non-ionizable in water. Consequently, it was anticipated that the only cationic charge involved in the electrostatic binding process with the DNA phosphate groups is the permanently charged pyridinium moiety.

Under acidic conditions, the methacrylate ester link is potentially hydrolysable. This was monitored by ^{1}H NMR spectroscopy. It was observed that even a drastic increase in temperature (80 °C), combined with a harsh acidic environment (pH $\sim$ 1), resulted in no change in the ^{1}H NMR spectrum, probably because of the stability of the polyamphiphile superstructures in H_2O (see the next section) that protect the ester link. These experiments suggest that the structural integrity of the P*n*DMAP-X in the form of micelles should not be affected by the acidic conditions prevailing in the endosome.

Aggregation behavior of P*n*DMAP-X in H_2O

The aggregation of P*n*DMAP-X in water before complexation was expected to have an impact on their interaction with DNA. This was examined first by the visual observation of P*n*DMAP-X aqueous solutions at two different concentrations,

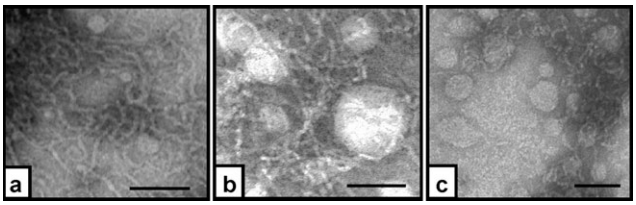

Fig. 2 Representative negative stain TEM images showing the morphology of the amphiphilic polymethacrylates prepared from solutions at the concentrations indicated: (a) P16DMAP-S8 (3.4 mg mL^{-1}; ×175 000; bar = 100 nm), (b) P16DMAP-S8 (0.5 mg mL^{-1}; ×175 000; bar = 100 nm) and (c) P12DMAP-S8 (0.5 mg mL^{-1}; ×175 000; bar = 50 nm).

low (0.5 mg mL^{-1}) and high (3–5 mg mL^{-1}). Solutions of the short spacer P*n*DMAP-X (*n* = 8; X = Br, S8) appeared transparent and thus soluble at all of the concentrations tested. They were also quite viscous in high concentrations. Low concentrations of the longer spacer P*n*DMAP-X (*n* = 12, 16; X = Br, S8) were also transparent; however, high concentrations were turbid, indicating the presence of suspensions large enough to scatter light. An increase in temperature during sonication enhanced their solubility somewhat, but without completely eliminating the turbidity. Furthermore, after both cold storage (4 °C) and lengthy periods at room temperature, gels were easily visible. This was most evident for P12DMAP-X, which was polymerized without transfer agent, compared to P16DMAP-X, polymerized in the presence of transfer agent—probably a consequence of the higher molar mass of the former, as explained in previous publications.[29,31]

The negative stain TEM technique allows direct observations of P*n*DMAP-X morphologies, which were investigated at low and high concentrations (0.5 and 3.4 mg mL^{-1}, respectively). Representative images are shown in Fig. 2. The images obtained from high concentrations of P*n*DMAP-X (*n* = 12 and 16) were characterized by a mixture of worm-like and spherical micelles (Fig. 2a for P16DMAP-S8). The diameters of the spherical micelles of P16DMAP-S8 were 20–70 nm and the tube diameters about 6 nm. Similar shapes were observed for the more dilute solutions (0.5 mg mL^{-1}) of the longer spacer polyamphiphiles (*n* = 12 and 16). All P*n*DMAP-X structures studied had tube diameters of 5–7 nm, whereas the diameters of the spherical micelles varied widely from about 20 to 130 nm, as shown for P*n*DMAP-S8 (*n* = 12, 16) in Fig. 2b and c. For P8DMAP-X, aggregates also appeared to be present at both low and high concentrations, but they were barely visible and their shape was poorly defined (images not shown). The TEM observations thus indicate that all of the P*n*DMAP-X presented some degree of aggregation in both the dilute and concentrated solutions investigated, even those that were visually transparent.

Complexation of P*n*DMAP-X with DNA

To evaluate the capability of P*n*DMAP-X to neutralize DNA, agarose gel shift assays were performed. The observation of complete gel retardation of DNA usually indicates that charge neutralization of DNA has been achieved. Fig. 3 shows representative images of agarose gel electrophoresis

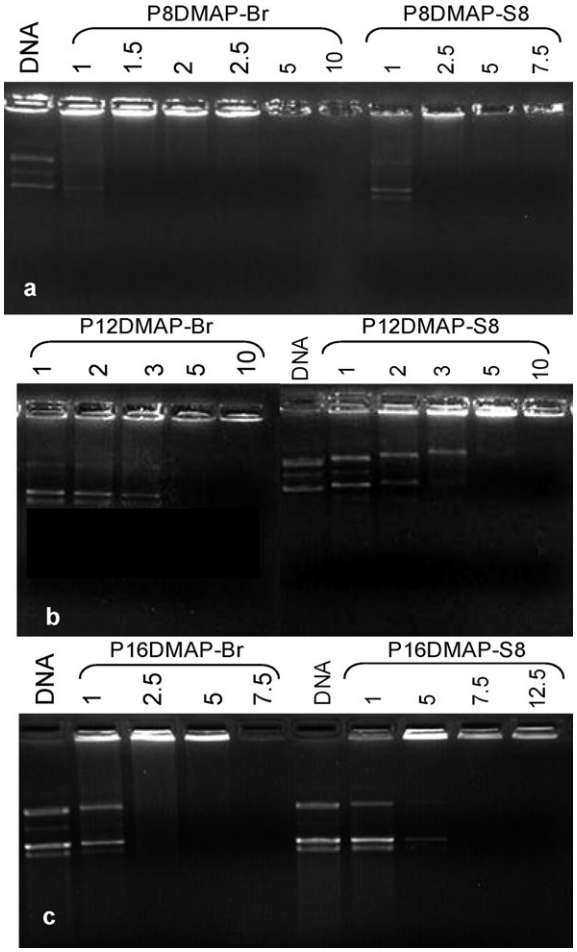

Fig. 3 Representative gel electrophoresis shift assays of the P*n*DMAP-X-based polyplexes with pBudCE4.1/LacZ/CAT plasmid. Wells were loaded with the equivalent of 400 ng of DNA. Naked DNA was used as a control.

for P*n*DMAP-X/DNA polyplexes formed at different weight ratios. Naked DNA was used as a control. The images suggest that complete neutralization of the negative charge (phosphate groups) of plasmid DNA can indeed be achieved by the positive charges (pyridinium moieties) of P*n*DMAP-X. For P8DMAP-X and P12DMAP-X, the minimum weight ratios required were about 1.5 and 3–5, respectively, whereas for P16DMAP-X, weight ratios of 2.5–5 and 5–7.5 for X = Br and S8, respectively, were necessary. Table 1 gives the charge ratios corresponding to the weight ratios, showing that the decrease in charge density of P*n*DMAP-X with increase in spacer length cannot account for the differences in minimum weight ratio necessary to achieve complete gel retardation. This indicates that the amount of P*n*DMAP-X required to arrest DNA migration increases with spacer length. Any dependence on the nature of the counterion is less clear, except for *n* = 16, where a higher weight ratio appears necessary, more for S8 than for bromide.

Fig. 3 also suggests that the degree of DNA condensation depends on the spacer length. For instance, a marked fluorescence on the anode side of the loading wells can be observed for P16DMAP-X at weight ratios ≥ 5. This might

Table 1 Size distributions and ζ-potentials of P*n*DMAP-X/DNA polyplexes of various weight and molar charge ratios, as determined by DLS

	Ratios		Distribution (intensity)		Distribution (number)	
Polymer	w/w	±[a]	Size (SD)/nm[b]	PDI/nm[c]	Size (SD)/nm[b]	ζ-potential/mV
P8DMAP-Br	1	0.9	383 (25)	0.26	147 (8)	−24
	1.5	1.3	171 (6)	0.24	73 (4)	15
P8DMAP-S8	1	0.7	141 (20)	0.22	62 (5)	−37
	1.5	1.0	179 (11)	0.23	94 (7)	8
P12DMAP-Br	2	1.6	175 (8)	0.19	96 (7)	−25
	2.5	1.9	198 (14)	0.39	44 (3)	−21
P12DMAP-S8	3	1.9	217 (33)	0.23	103 (14)	16
	5	3.1	141 (9)	0.21	69 (5)	19
P16DMAP-Br	3.5	2.4	124 (3)	0.17	64 (4)	25
	5	3.5	172 (12)	0.36	49 (2)	36
P16DMAP-S8	7.5	4.2	175 (9)	0.26	85 (13)	−52
	10	5.7	394 (54)	0.33	170 (23)/73 (16)	−18
	12	6.8	343 (21)	0.42	156 (15)/72 (17)	29

[a] Molar ratios of charges (±) were calculated supposing that the small counterions [Br or S8 for aPPs, Na and Mg (assuming a proportion of 50 : 50 Na : Mg w/w) for DNA] remain present in the polyplexes. If these counterions are totally absent, the ratios are only slightly modified: *e.g.*, for the P8DMAP-Br/DNA polyplex of 0.9 charge ratio, with the small counterions present as specified, becomes exactly equimolar (1.0 charge ratio) if no small counterions are present. [b] SD = standard deviation. [c] PDI = polydispersity index.

indicate that DNA was imperfectly condensed, meaning that ethidium bromide could still diffuse within the DNA strands in the complex. A similar behavior was reported for hydrophobized and highly charged PAMAM.[13] Within the P*n*DMAP-Br series, the fluorescence in the loading wells appears more intense for $n = 8$ and 16 than for $n = 12$. In contrast, within the P*n*DMAP-S8 series, $n = 8$ showed the lowest fluorescence intensity in the wells.

ζ-potential of the polyplexes

It has been observed that non-specific absorptive endocytosis of nanoparticles formed from cationic polymers is possible with positively-charged complexes.[34] To determine the influence of the surface charge of P*n*DMAP-X polyplexes on the transfection efficiency, the ζ-potentials of the polyplexes were measured. The data are given in Table 1. Polyplexes prepared from the shorter spacer polyamphiphiles ($n = 8$) present charge inversion between weight ratios of 1 and 1.5 (or ± a charge ratio of ~1). The ratio for charge inversion tends to increase with spacer length [at least for P12DMAP-Br, where it occurs above a weight ratio of 2.5 (± ratio of ~2), and for P16DMAP-S8, where it occurs between weight ratios of 10 and 12 (± ratio of ~6)]. A clear difference between the bromide and S8 counterions was observed only for $n = 16$, with charge inversion occurring at a much lower ratio for bromide than for S8. In fact, the polyplex with P16DMAP-S8 stood out with the very high ratio required for its ζ-potential charge inversion, which was, furthermore, much higher than that required to completely retard DNA. In contrast, the ζ-potential charge inversion for $n = 8$ (and possibly $n = 12$, although this was less evident) was consistent with that required for complete retardation of DNA migration in gel electrophoresis.

Size of the polyplexes by DLS

Previous investigations have suggested that polycations capable of compacting DNA into stable nanoparticles (<200 nm) allow effective entry of the polyplexes into the cell through an endocytosis mechanism[35] and promote intracellular trafficking.[36] With this in mind, we used DLS to determine the sizes (hydrodynamic radii) of the various polyplexes. Data obtained from the number distribution curve given in Table 1 indicate that all of the aPPs studied can condense DNA into relatively small particles of generally less than 100 nm. Polyplexes with the smallest diameters (44 nm) were formed from P12DMAP-Br at a weight ratio of 2.5. All polyplexes were characterized by a large polydispersity index (>0.17), indicating a broad size distribution. In two cases, for P16DMAP-S8/DNA polyplexes at weight ratios of 10 and 12, the number distribution curve was bimodal, which can be attributed to a small amount of particle aggregation (see the TEM image in Fig. 5f, where many interconnections between particles are visible). This was not observed in the intensity distribution curve because large objects scatter light much more strongly than small ones, resulting in much more weight given to the larger particles. In comparison, the bimodal number distribution of sizes demonstrates the coexistence of a small proportion of aggregates and a predominant fraction of small-sized particles. On the other hand, the validity of the DLS experiments on these suspensions might be questioned given the non-spherical aspect of a significant portion of the objects, as observed by TEM (see the next section). For instance, flexible and non-condensed DNA [see the TEM observations of P8DMAP-X polyplexes (w/w = 1)] should scatter light less extensively than condensed DNA (Fig. 4a).[37] Nevertheless, the sizes obtained by light scattering data were in good agreement with those obtained by TEM.

Morphology of the polyplexes determined by TEM

According to previous investigations,[36] the degree of compaction of the plasmid DNA and the morphology (spherical/toroidal) of the particles are critical factors in transfection efficiency. In the present study, TEM observations were used to observe the morphologies and to confirm the sizes of polyplexes obtained by DLS measurements. Representative TEM images of freshly prepared polyplexes are presented in Fig. 4 and Fig. 5.

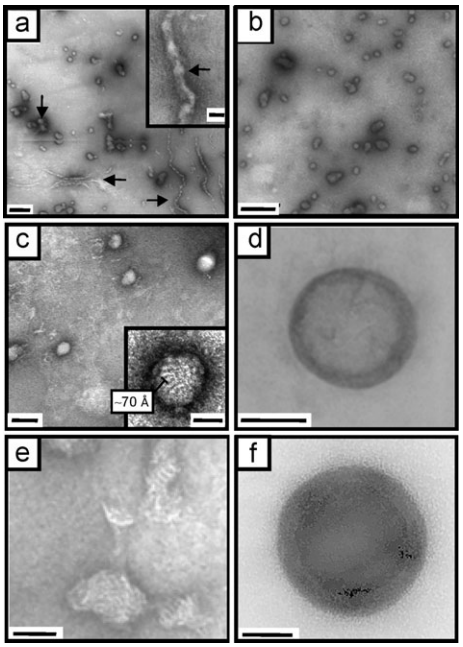

Fig. 4 Representative negative stain TEM images showing the morphologies of the P*n*DMAP-Br/DNA polyplexes: (a) $n = 8$, ratio (w/w) = 1 (×37 500, bar = 200 nm); arrows point to aggregated nanoparticles and fibrillar-like objects; the inset shows the magnification of one incompletely-condensed DNA fragment (×175 000, bar = 25 nm); (b) $n = 8$, ratio (w/w) = 5 (×37 500, bar = 200 nm); (c) $n = 12$, ratio (w/w) = 2.5 (×62 500, bar = 100 nm), the insert shows the magnification of a nanoparticle with internal lamellar-like order (×230 000, bar = 50 nm); (d) $n = 12$, ratio (w/w) = 2.5 (×300 000, bar = 100 nm); (e) $n = 16$, ratio (w/w) = 5 (×175 000, bar = 50 nm); (f) $n = 16$, ratio (w/w) = 5 (×105 000, bar = 100 nm).

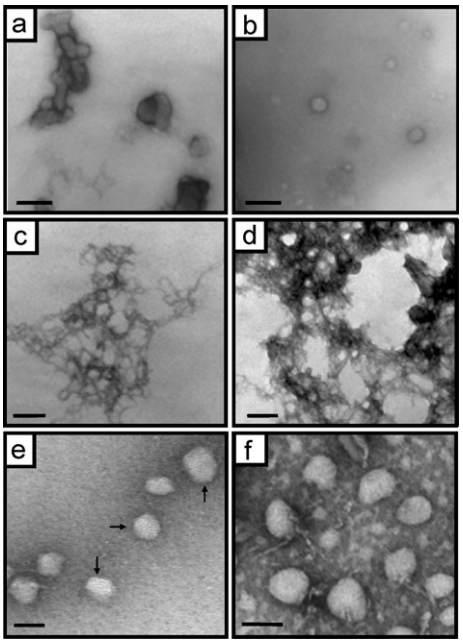

Fig. 5 Representative negative stain TEM images showing the morphology of the P*n*DMAP-S8/DNA polyplexes (bar = 100 nm, unless otherwise mentioned): (a) $n = 8$, ratio (w/w) = 1 (×62 500); (b) $n = 8$ ratio (w/w) = 2.5 (×62 500); (c) $n = 12$, ratio (w/w) = 1 (×62 500); (d) $n = 12$, ratio (w/w) = 2.5 (×62 500); (e) $n = 16$, ratio (w/w) = 10 (×175 000, bar = 50 nm), arrows indicate particles with internal order; (f) $n = 16$, ratio (w/w) = 10 (×175 000).

P*n*DMAP-Br series. P8DMAP-Br/DNA polyplexes formed at a weight ratio of 1, for which there is incomplete neutralization, appeared as a mixture of different morphologies (Fig. 4a). Particles with roughly spherical shapes and small sizes (~50 nm), as well as particles with a fibril-like morphology, were clearly visible throughout the preparation. These particles were either isolated (see inset in Fig. 4a) or in the form of bundles, and were reminiscent of the morphology reported for functional PAMAM.[38] This morphology cannot be attributed to free DNA, since the diameters of the small thread-like objects (axial diameter ~25 nm) was not commensurate with the thickness of the DNA double helix (2.55 nm for the B-DNA form).[39] It is likely that this structure is the result of incomplete condensation of the DNA due to partial neutralization of the phosphate groups by the pyridinium moieties at this weight ratio, in accordance with the ζ-potential data. Moreover, a small proportion of the particles visible in Fig. 4a were aggregated. An increase in the proportion of P8DMAP-Br to weight ratios of ~2.5 (not shown in Fig. 4) and 5 resulted in the formation of positive complexes and lead to a better compaction of DNA with a more uniform particulate morphology and with sizes ranging from 35 to 50 nm (Fig. 4b). In this case, there were no visible interconnections between surface-charged particles.

As shown in Fig. 4c–f, polyplexes formed from both P12DMAP-Br and P16DMAP-Br also showed mixed morphologies. For P12DMAP-Br, at a weight ratio of 2.5, the predominant form was small, spherical particles of ~43 nm (Fig. 4c), in accordance with the DLS data; they were characterized by an internal lamellar-like structure with a repeat distance of ~7 nm (see insert of Fig. 4c). For P16DMAP-Br (investigated at a weight ratio of 5.0), the particles were 50–100 nm in size, but generally not spherical (Fig. 4e). In addition, particles with a toroidal-like morphology, of diameter 100–125 nm for P12DMAP-Br (Fig. 4d) and ~290 nm for P16DMAP-Br (Fig. 4f), were occasionally observed. This is worthy of mention because, to our knowledge, this is the first observation of these structures in polymethacrylate systems, whereas they have been reported for other polymeric systems[13,40–42] and small polyamine molecules.[43]

P*n*DMAP-S8 series. The TEM images of P8DMAP-S8 polyplexes at weight ratios of 1 and 2.5, shown in Fig. 5a–b, reveal the presence of heterogeneous DNA structures with incompletely condensed DNA, as well as uniform particles. For the polyplexes based on P12DMAP-S8 and P16DMAP-S8, TEM observations indicate, in accordance with the gel electrophoresis results, that a larger amount of polyamphiphile is necessary to condense DNA into small and well-defined particles. The images for the P12DMAP-S8 polyplexes in Fig. 5c–d show that well-defined condensed particles were not attained for a weight ratio of 2.5, contrasting with the P12DMAP-Br polyplex at the same weight ratio. In contrast, a weight ratio of 10 for P16DMAP-S8 polyplexes did

result in the formation of well-defined particles (~50 nm), which, moreover, showed an internal structure in some cases.

Thus, a common trend indicated by the TEM images of the various P*n*DMAP-X polyplexes (Fig. 4 and Fig. 5) is the increased ratio of polyamphiphile necessary for the development of small-sized spherical nanoparticles as the spacer length increases. On the other hand, at any given weight ratio, the substitution of bromide counterions by S8 counterions had a tendency to decrease the ability of the polyamphiphiles to efficiently condense DNA and generate discrete well-defined nanoparticles.

Cytotoxicity of the P*n*DMAP-X polyamphiphiles

The variations of the *in vitro* cell cytotoxicity observed for the two series of polyamphiphiles are presented in Fig. 6 and compared with the cytotoxicity of branched PEI. The cytotoxicity is expressed as the relative percentage of metabolically-active cells as a function of the aPP concentration, which varied from 1.5 to 22.5 μg mL^{-1}.

At a given concentration, the P*n*DMAP-X polyamphiphiles were always less cytotoxic than PEI. For example, at a polymer concentration of 3.75 μg mL^{-1} (equivalent to the concentration of the polycation in a polyplex of weight ratio 2.5), 85–90% of the cells were still viable, compared to less than 50% viability for cells treated with PEI. In the P*n*DMAP-Br series, the cytotoxicity depended on the spacer length, the longest spacer aPPs ($n = 16$) being significantly more cytotoxic ($p < 0.05$) than the shorter spacers aPPs ($n = 8$, 12). The P*n*DMAP-S8 series showed a similar, although more weak, relationship of cytotoxicity to spacer length. The nature of the counterion also affected the cytotoxicity profile of the polyamphiphile, but there was no general trend. However, at high concentrations of polyamphiphile (22.5 μg mL^{-1}; 7.5–22.5 for $n = 16$), the cell viability was higher for S8 than for bromide ($p < 0.05$).

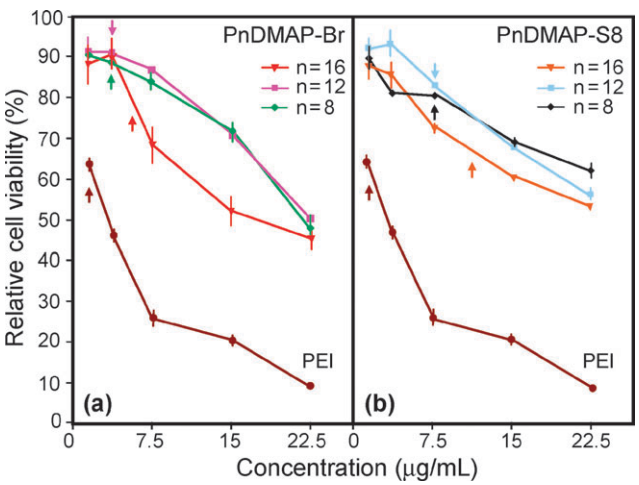

Fig. 6 The relative cell viability of the COS7 cells after 24 h exposure as a function of the polycation concentration for the P*n*DMAP-X polyamphiphiles in comparison with PEI. Cells treated with (a) P*n*DMAP-Br and (b) P*n*DMAP-S8. Arrows indicate the concentration corresponding to optimal transfection efficiency for each polycation. Bars indicate standard deviations.

In vitro transfection efficiency of polyplexes

The impact of the counterion, spacer length and weight ratio complexation on the *in vitro* transfection efficiency was also examined. Naked DNA and PEI-based polyplexes were employed as negative and positive controls, respectively. Fig. 7 displays the transfection efficiencies of the various polyplexes. The expression level of the transgene as a function of the ratio employed appeared as a bell-shaped profile for all of the aPPs tested. The maximum transfection efficiency was obtained for polyplexes with P12DMAP-Br at a weight ratio of 2.5 (charge ratio of 1.9). Its value was much higher than that of any of the other P*n*DMAP-X polyplexes (more than 5 times higher than the next best example, P12DMAP-S8 at a w/w = 5) and of the same order of magnitude as that generated by PEI polyplexes (N : P = 10).

Within the P*n*DMAP-Br series, the optimum weight ratio for transfection varied with spacer length, ranging from 2.5 for $n = 8$ and $n = 12$ to 3.75 for $n = 16$. Moreover, the transfection efficiency was highest for $n = 12$, followed by $n = 8$, with $n = 16$ giving much poorer results. Within the P*n*DMAP-S8 series, the optimum weight ratios for transfection ranged from 5 for $n = 8$ and $n = 12$ to 7.5 for $n = 16$. Thus, the optimum transfection occurred at higher weight ratios in the S8 series compared to the bromide homologues. The transfection efficiency as a function of spacer length followed the same trend in both series ($12 > 8 > 16$), although the differences were much less marked in the S8 series. Additional weight ratio optimization may possibly further improve the transfection efficiency of the P*n*DMAP-X/DNA polyplexes.

Discussion

Tail-end amphiphilic polymethacrylates with different spacer lengths and counterions [inorganic (bromide) *vs.* organic (octylsulfonate)] were investigated, and evaluated for plasmid DNA condensation, cell cytotoxicity and *in vitro* transfection efficiency. Both spacer length and the nature of the counterion were found to have significant impacts on the physicochemical and biological characteristics of the resulting polyplexes.

Physicochemical properties of the polyplexes

All of the P*n*DMAP-X polyamphiphiles neutralize and condense DNA *via* electrostatic interactions between negatively-charged DNA phosphate groups and positively-charged dimethylaminopyridinium "tail-end" groups. This concords with several studies that have demonstrated that permanently charged polycations (ammonium or pyridinium)[15] are better condensing agents than protonable polycations, whose charge density is pH-dependent.[44] Moreover, the position of the cationic charge near the end of a flexible side chain makes it more accessible, which probably facilitates electrostatic interactions with the DNA.

This investigation indicates that an increase in spacer length and, for P16DMAP-X, the use of long counterions (S8) decreases the efficiency of the neutralization and condensation processes. This is the first reported evidence of the effect of the chemical nature of counterions (for permanently charged

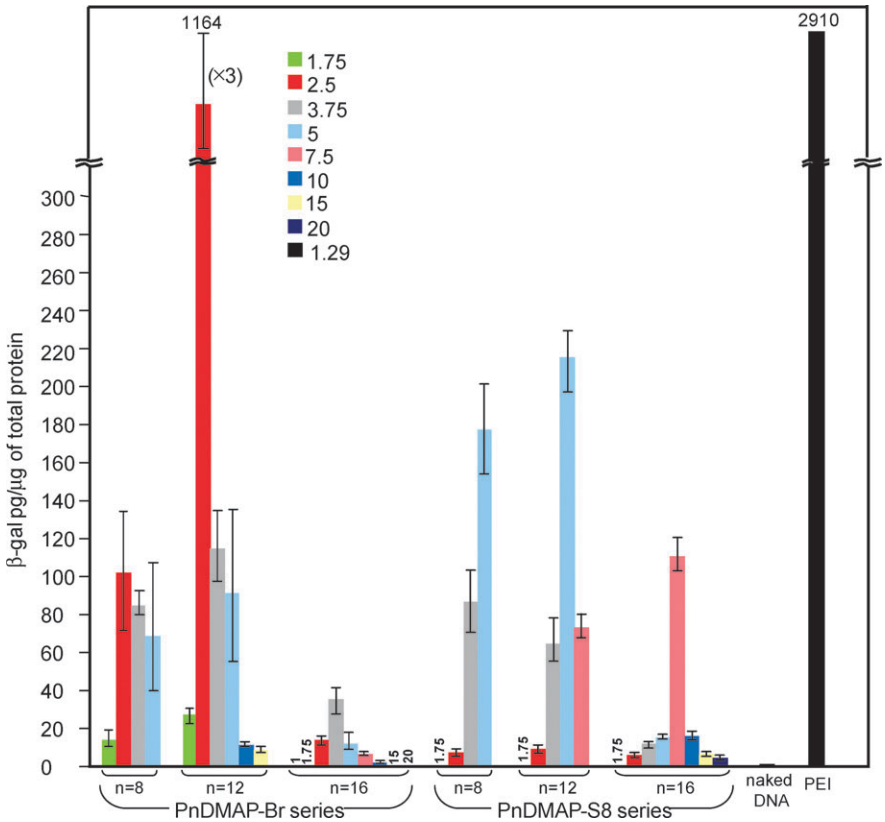

Fig. 7 The transfection of COS7 cells using the plasmid pBudCE4.1/LacZ/CAT complexed with various P*n*DMAP-X polyamphiphiles in the weight ratio range 1–20. Bars indicate standard deviations. A weight ratio of 1.29 (corresponding to N : P = 10) was used for the preparation of PEI-based polyplexes.

polycations) on the neutralization and physical structure of polyplexes. The spacer effect could be attributable, at least in part, to the change in the overall hydrophilic/hydrophobic balance of the P*n*DMAP-X, which dictates the structural organization of P*n*DMAP-X in solution and thereby influences subsequent electrostatic interactions with DNA. For example, the lack of well-defined and thus more soluble micellar superstructures of P8DMAP-X in solution could explain their more efficient neutralization at lower polymer/DNA weight ratios compared with the longer spacer aPPs (n = 12 and 16). These latter complexes have well-defined micellar superstructures in solution, in which the cation may be less available for interaction, thus requiring higher amounts of P*n*DMAP-X for efficient DNA neutralization and condensation. On the other hand, the S8 counterion can reduce the accessibility of the pyridinium group due to its size and/or the hydrophobicity of its alkyl chain.

Biophysical characteristics of the polyamphiphiles and polyplexes

The influence of the structural characteristics of polyamphiphiles on cell viability is still poorly understood, despite extensive investigations.[13,34,45] The combination of characteristics such as the cationic charge[46] and the presence of lipid-like segments[47] can result in acute cytotoxicity. In particular, as we reported elsewhere,[13] the covalent attachment of aliphatic segments to a permanently charged PAMAM backbone is detrimental to cell viability due to a detergent effect on the cell membrane. Within the P*n*DMAP-X series, the combination of aliphatic side chain spacers and quaternized DMAP terminal groups led to only mild cytotoxicity. Furthermore, P*n*DMAP-X polyamphiphiles were much less cytotoxic than PEI (branched, 25 kDa). High cationic charge density is generally suspected when notable cell cytotoxicity is observed. The molar ratio of charges for a weight ratio of 1 for aPPs varied between 1 for P8DMAP-Br and 0.56 for P16DMAP-S8 (see Table 1), compared to 0.9 for PEI at physiological pH (only 20% of amine groups are protonated).[42,48] Consequently, the weak cytotoxicity of the polyamphiphiles cannot be explained by a low charge density. The "tail-end geometry" of the P*n*DMAP-X polyamphiphiles that is responsible for micelle formation may account for the weak cytotoxicity by masking the hydrophobic segments of P*n*DMAP-X. It is further possible that the rigidity of the terminal pyridinium fragments decreases the detergent effect of the aPPs. The latter is supported by observations reported for nitrogen-containing heterocycle polycations[49] and surfactants,[50] indicating that pyridinium head groups have little impact on cytotoxicity because they limit interactions with the cell membrane.

In many instances, high cytotoxicity interferes with the transfection process and can explain differences in transfection efficiency between gene delivery systems.[51,52] Given the relatively low cytotoxicity of all of the P*n*DMAP-X

polyamphiphiles, the differences observed in transfection efficiency should not be attributed to this factor, but mainly to physicochemical characteristics.

In terms of the potential of the aPPs as new gene transfer agents, the present investigation indicates that the spacer length and the nature of the counterion, in addition to the aPP/DNA weight (or charge) ratio, strongly influence the level of transfection. In general, a small size, a regular shape (spherical/toroidal) and a net positively-charged surface are considered to be essential characteristics for efficient gene transfer into cells.[34–36] Other factors, such a endosomal buffering capacity,[11,53] an appropriate association and dissociation strength between the DNA and polycations,[10,54] and the stability of the polyplexes in solution[55] are also important for efficient gene transfer. In the present study, maximum transfection efficiency occurred at a particular weight ratio for each P*n*DMAP-X polyamphiphile tested, which may correspond to optimal physicochemical properties for the transfection process. Furthermore, good transfection efficiencies were obtained from formulations where an excess of polyamphiphile was present.[56]

On the other hand, this work demonstrates that a positive surface charge of polyplexes based on P*n*DMAP-X is not crucial for high transfection efficiency, as was also observed for carboxylated poly(amidoamine)s[38,57,58] and, to a lesser extent, functional poly(histidine)s.[59] Indeed, the only P*n*DMAP-X polyamphiphile of those investigated that competes with PEI as a gene transfer agent, P12DMAP-Br at w/w = 2.5, has a negative surface charge (−21 mV) [in the P16DMAP-S8 series, the w/w ratio giving the highest transfection efficiency also had a negative surface charge (−52 mV)]. The P12DMAP-Br-based polyplexes at w/w = 2.5 also formed stable particles of small size (*ca.* 45 nm) and with a well-defined morphology.

To rationalize in part why P12DMAP-Br of weight ratio 2.5 is by far the most efficient gene delivery agent of all the aPPs investigated, reference can be made to previous reports on amphiphilic poly(methacrylate)s,[60] poly(vinylpyridine)s[61] and, more recently, poly(ethyleneimine),[17] which demonstrate that interactions between polyplexes and the cell membrane depend on the length of the alkyl side chain. In the case of P*n*DMAP-X, the amphiphilic character was modulated by the spacer length and counterion size. A spacer length of $n = 8$ may be too short to destabilize the cell membrane, whereas a spacer length of $n = 16$ caused major cell membrane disruption that was reflected in the increased cytotoxicity. A polyamphiphile possessing a spacer with twelve CH_2 units may thus represent the optimum length that allows for an appropriate hydrophilic/hydrophobic balance, and for the most efficient non-specific lipophilic interaction with the cell membrane. These remarks appear to be in agreement with the conclusions for hydrophobized (branched) PEI reported by Doody and co-workers.[17]

On the other hand, the polyplex-mediated gene transfection process is complex and incompletely understood, even in the best-studied systems. The fact that one example of the present system has a transfection efficiency competitive with that of PEI demonstrates its potential as an effective gene transfection agent that merits further study. This is all the more true because their tail-end architecture, combining polymer and surfactant character, is novel for gene transfection agents. Besides the demonstration of their interest for gene transfection applications, this study has made a start at correlating the physicochemical and biological characteristics of these particular types of polyplexes. Given the limited number of parameters investigated and the many other parameters that may be varied (in particular, molar mass and other molecular parameters), it may be expected that conditions for still higher transfection efficiencies may be found. In the course of further study, the novel architecture involved may also provide new insights into the transfection process in general.

Conclusions

This study describes a novel family of amphiphilic "tail-end" polymethacrylates with pyridinium cationic charges that potentiate efficient gene delivery. Both the spacer length and the nature of the counterion influence the physicochemical characteristics of the polyplexes and their transfection efficiencies. Negatively-charged polyplexes were able to transfect cells at a level similar to PEI-based polyplexes, and do this while being less cytotoxic. This contrasts with the general belief that polyplexes characterized by a high positive ζ-potential are essential for gene transfer. Finally, this family of tail-end polyamphiphiles is of interest, not only for its promise as a gene transfection agent, but also because a number of structural parameters can be easily modified (aliphatic spacer length, nature of the counterion, type of pyridinium group[16,19,20]) to both optimize their activity and study transfection mechanisms. In addition, copolymers could also be envisaged,[62] including in the form of a mixture of counterions.

Acknowledgements

This work was supported by Valorisation Recherche Québec (Gouvernement du Québec, Project number: 2201-141). We are thankful to D. Montpetit (Agriculture et Agroalimentaire Canada, Centre de Recherche et de Développement sur les Aliments, Saint-Hyacinthe (QC)) for her invaluable help with transmission electron microscopy and N. Robert (Centre de Recherche et de Développement sur les Aliments, Saint-Hyacinthe (QC)) for his technical contribution to the gel electrophoresis experiments. Discussions with Dr A. Morphesis from Malvern were highly appreciated. P. Y. V. thanks Agriculture et Agroalimentaire Canada, Centre de Recherche et de Développement sur les Aliments, Saint-Hyacinthe (QC) for technical support.

Notes and references

1 A. V. Kabanov, P. Lemieux, S. Vinogradov and V. Alakhov, *Adv. Drug Delivery Rev.*, 2002, **54**, 223.
2 E. Wagner and J. Kloeckner, *Adv. Polym. Sci.*, 2006, **192**, 135.
3 T. Merdan, J. Kopecek and T. Kissel, *Adv. Drug Delivery Rev.*, 2002, **54**, 715.
4 S. K. Mendiratta, A. Quezada, M. Matar, J. Wang, H. L. Hebel, S. Long, J. L. Nordstrom and F. Pericle, *Gene Ther.*, 1999, **6**, 833.
5 P. Lemieux, N. Guerin, G. Paradis, R. Proulx, L. Chistyakova, A. Kabanov and V. Alakhov, *Gene Ther.*, 2000, **7**, 986.

6 B. Martin, M. Sainlos, A. Aissaoui, N. Oudrhiri, M. Hauchecorne, J. P. Vigneron, J. M. Lehn and P. Lehn, *Curr. Pharm. Des.*, 2005, **11**, 375.
7 P. C. Bell, M. Bergsma, I. P. Dolbnya, W. Bras, M. C. A. Stuart, A. E. Rowan, M. C. Feiters and J. Engberts, *J. Am. Chem. Soc.*, 2003, **125**, 1551.
8 S. Denoyelle, A. Polidori, P. Y. Vuillaume, M. Brunelle, S. Laurent, Y. El Azhary and B. Pucci, *New J. Chem.*, 2006, **30**, 629.
9 M. Brunelle, A. Polidori, S. Denoyelle, A. S. Fabiano, P. Y. Vuillaume, S. Laurent-Lewandowski and B. Pucci, *C. R. Chim.*, 2009, **12**, 188.
10 A. N. Zelikin, E. S. Trukhanova, D. Putnam, V. A. Izumrudov and A. A. Litmanovich, *J. Am. Chem. Soc.*, 2003, **125**, 13693.
11 O. Boussif, F. Lezoualch, M. A. Zanta, M. D. Mergny, D. Scherman, B. Demeneix and J. P. Behr, *Proc. Natl. Acad. Sci. U. S. A.*, 1995, **92**, 7297.
12 A. N. Zelikin, D. Putnam, P. Shastri, R. Langer and V. A. Izumrudov, *Bioconjugate Chem.*, 2002, **13**, 548.
13 P. Y. Vuillaume, M. Brunelle, M. R. Van Calsteren, S. Laurent-Lewandowski, A. Begin, R. Lewandowski, B. G. Talbot and Y. ElAzhary, *Biomacromolecules*, 2005, **6**, 1769.
14 M. Thomas and A. M. Klibanov, *Proc. Natl. Acad. Sci. U. S. A.*, 2002, **99**, 14640.
15 A. V. Kabanov, I. V. Astafyeva, M. L. Chikindas, G. F. Rosenblat, V. I. Kiselev, E. S. Severin and V. A. Kabanov, *Biopolymers*, 1991, **31**, 1437.
16 V. A. Kabanov, A. V. Kabanov and I. N. Astavieva, *Polym. Reprints*, 1991, **32**, 592.
17 A. M. Doody, J. N. Korley, K. P. Dang, P. N. Zawaneh and D. Putnam, *J. Controlled Release*, 2006, **116**, 227.
18 M. D. Brown, A. Schatzlein, A. Brownlie, V. Jack, W. Wang, L. Tetley, A. I. Gray and I. F. Uchegbu, *Bioconjugate Chem.*, 2000, **11**, 880.
19 A. Akinc, D. M. Lynn, D. G. Anderson and R. Langer, *J. Am. Chem. Soc.*, 2003, **125**, 5316.
20 A. Laschewsky, *Adv. Polym. Sci.*, 1995, **124**, 1.
21 M. Scarzello, J. Smisterova, A. Wagenaar, M. C. A. Stuart, D. Hoekstra, J. Engberts and R. Hulst, *J. Am. Chem. Soc.*, 2005, **127**, 10420.
22 M. Scarzello, V. Chupin, A. Wagenaar, M. C. A. Stuart, J. Engberts and R. Hulst, *Biophys. J.*, 2005, **88**, 2104.
23 R. Hulst, I. Muizebelt, P. Oosting, C. van der Pol, A. Wagenaar, J. Smisterova, E. Bulten, C. Driessen, D. Hoekstra and J. Engberts, *Eur. J. Org. Chem.*, 2004, 835.
24 D. Pijper, E. Bulten, J. Smisterova, A. Wagenaar, D. Hoekstra, J. Engberts and R. Hulst, *Eur. J. Org. Chem.*, 2003, 4406.
25 A. Roosjen, J. Smisterova, C. Driessen, J. T. Anders, A. Wagenaar, D. Hoekstra, R. Hulst and J. Engberts, *Eur. J. Org. Chem.*, 2002, 1271.
26 J. M. Kuiper, R. T. Buwalda, R. Hulst and J. Engberts, *Langmuir*, 2001, **17**, 5216.
27 A. A. P. Meekel, A. Wagenaar, J. Smisterova, J. E Kroeze, P. Haadsma, B. Bosgraaf, M. C. A. Stuart, A. Brisson, M. H. J. Ruiters, D. Hoekstra and J. Engberts, *Eur. J. Org. Chem.*, 2000, 665.
28 A. Wagenaar, J. Smisterova, D. Hoekstra and J. Engberts, *Abstr. Pap. Am. Chem. Soc.*, 1999, **218**, U432.
29 P. Y. Vuillaume, C. G. Bazuin and J. C. Galin, *Macromolecules*, 2000, **33**, 781.
30 P. Y. Vuillaume and C. G. Bazuin, *Macromolecules*, 2003, **36**, 6378.
31 P. Y. Vuillaume, X. Sallenave and C. G. Bazuin, *Macromolecules*, 2006, **39**, 8339.
32 M. Z. von Schmoluchowsky, *Phys. Chem.*, 1917, **92**, 129.
33 P. Forsythe, R. Frampton, C. D. Johnson and A. R. Katritzky, *J. Chem. Soc., Perkin Trans. 2*, 1972, 671.
34 D. G. Anderson, A. Akinc, N. Hossain and R. Langer, *Mol. Ther.*, 2005, **11**, 426.
35 W. Zauner, M. Ogris and E. Wagner, *Adv. Drug Delivery Rev.*, 1998, **30**, 97.
36 H. Pollard, J. S. Remy, G. Loussouarn, S. Demolombe, J. Behr and D. Escande, *J. Biol. Chem.*, 1998, **273**, 7507.
37 See: *Self-Assembling Complexes for Gene Delivery: From Laboratory to Clinical Trial*, ed. A. V. Kabanov, P. L. Felgner and L. W. Seymour, John Wiley & Sons, New York, 1998 and references therein.
38 S. C. W. Richardson, N. G. Pattrick, Y. K. S. Man, P. Ferruti and R. Duncan, *Biomacromolecules*, 2001, **2**, 1023.
39 V. A. Kabanov, V. G. Sergeyev, O. A. Pyshkina, A. A. Zinchenko, A. B. Zezin, J. G. H. Joosten, J. Brackman and K. Yoshikawa, *Macromolecules*, 2000, **33**, 9587.
40 R. Golan, L. I. Pietrasanta, W. Hsieh and H. G. Hansma, *Biochemistry*, 1999, **38**, 14069.
41 M. Wittmar, J. S. Ellis, F. Morell, F. Unger, J. C. Schumacher, C. J. Roberts, S. J. B. Tendler, M. C. Davies and T. Kissel, *Bioconjugate Chem.*, 2005, **16**, 1390.
42 M. X. Tang and F. C. Szoka, *Gene Ther.*, 1997, **4**, 823.
43 I. Baeza, P. Gariglio, L. M. Rangel, P. Chavez, L. Cervantes, C. Arguello, C. Wong and C. Montanez, *Biochemistry*, 1987, **26**, 6387.
44 M. A. Wolfert, P. R. Dash, O. Nazarova, D. Oupicky, L. W. Seymour, S. Smart, J. Strohalm and K. Ulbrich, *Bioconjugate Chem.*, 1999, **10**, 993.
45 H. T. Lv, S. B. Zhang, B. Wang, S. H. Cui and J. Yan, *J. Controlled Release*, 2006, **114**, 100.
46 K. A. Mislick and J. D. Baldeschwieler, *Proc. Natl. Acad. Sci. U. S. A.*, 1996, **93**, 12349.
47 A. A. Yaroslavov, S. A. Sukhishvili, O. L. Obolsky, E. G. Yaroslavova, A. V. Kabanov and V. A. Kabanov, *FEBS Lett.*, 1996, **384**, 177.
48 J. Suh, H. J. Paik and B. K. Hwang, *Bioorg. Chem.*, 1994, **22**, 318.
49 D. Fischer, Y. X. Li, B. Ahlemeyer, J. Krieglstein and T. Kissel, *Biomaterials*, 2003, **24**, 1121.
50 M. A. Ilies, B. H. Johnson, F. Makori, A. Miller, W. A. Seitz, E. B. Thompson and A. T. Balaban, *Arch. Biochem. Biophys.*, 2005, **435**, 217.
51 P. van de Wetering, J. Y. Cherng, H. Talsma and W. E. Hennink, *J. Controlled Release*, 1997, **49**, 59.
52 P. van de Wetering, J. Y. Cherng, H. Talsma, D. J. A. Crommelin and W. E. Hennink, *J. Controlled Release*, 1998, **53**, 145.
53 W. T. Godbey, K. K. Wu and A. G. Mikos, *Proc. Natl. Acad. Sci. U. S. A.*, 1999, **96**, 5177.
54 D. V. Schaffer, N. A. Fidelman, N. Dan and D. A. Lauffenburger, *Biotechnol. Bioeng.*, 2000, **67**, 598–606.
55 J. Luten, N. Akeroyd, A. Funhoff, M. C. Lok, H. Talsma and W. E. Hennink, *Bioconjugate Chem.*, 2006, **17**, 1077.
56 W. C. Shen and H. P. Ryser, *Proc. Natl. Acad. Sci. U. S. A.*, 1978, **75**, 1872.
57 P. Ferruti, S. Manzoni, S. C. W. Richardson, R. Duncan, N. Pattrick, G. R. Mendichi and M. Casolaro, *Macromolecules*, 2000, **33**, 7793.
58 J. Franchini, E. Ranucci and P. Ferruti, *Biomacromolecules*, 2006, **7**, 1215.
59 D. Putnam, A. N. Zelikin, V. A. Izumrudov and R. Langer, *Biomaterials*, 2003, **24**, 4425.
60 K. Kuroda and W. F. DeGrado, *J. Am. Chem. Soc.*, 2005, **127**, 4128.
61 J. C. Tiller, C.-J. Liao, K. Lewis and A. M. Klibanov, *Proc. Natl. Acad. Sci. U. S. A.*, 2001, **98**, 5981.
62 P. Y. Vuillaume, J. C. Galin and C. G. Bazuin, *Macromolecules*, 2001, **34**, 859.

